

The Role of Angular Momentum and Cosmic Censorship in the (2+1)-Dimensional Rotating Shell Collapse

Robert B. Mann^{a*}, John J. Oh^{b†}, and Mu-In Park^{c‡}

^a *Department of Physics and Astronomy, University of Waterloo,
Waterloo, Ontario, N2L 3G1, Canada*

^b *Division of Interdisciplinary Mathematics, National Institute for Mathematical Sciences,
Daejeon, 304-350, Korea*

^c *Research Institute of Physics and Chemistry, Chonbuk National University,
Chonju, 561-756, Korea*

Abstract

We study the gravitational collapse problem of rotating shells in three-dimensional Einstein gravity with and without a cosmological constant. Taking the exterior and interior metrics to be those of stationary metrics with asymptotically constant curvature, we solve the equations of motion for the shells from the Darmois-Israel junction conditions in the *co-rotating* frame. We study various collapse scenarios with *arbitrary* angular momentum for a variety of geometric configurations, including anti-de Sitter, de Sitter, and flat spaces. We find that the collapsing shells can form a BTZ black hole, a three-dimensional Kerr-dS spacetime, and an horizonless geometry of point masses under certain initial conditions. For pressureless dust shells, the curvature singularity is *not* formed due to the angular momentum barrier near the origin. However when the shell pressure is nonvanishing, we find that for all types of shells with polytropic-type equations of state (including the perfect fluid and the generalized Chaplygin gas), collapse to a naked singularity is *possible* under generic initial conditions. We conclude that in three dimensions angular momentum does not in general guard against violation of cosmic censorship.

PACS numbers: 04.20.Dw, 04.40.-b, 04.60.Kz, 04.70.Bw

Typeset Using L^AT_EX

*email:rbmann@sciborg.uwaterloo.ca

†email:johnoh@nims.re.kr

‡email:muinpark@gmail.com

1 Introduction

In three-dimensional Einstein gravity, there are no dynamical degrees of freedom, i.e., no gravitons that mediate the interactions between massive objects in the vacuum [1], with or without the cosmological constant, unless some higher derivative terms, like the (gravitational) Chern-Simons term, are introduced [2]. Although spacetime outside of matter is locally of constant curvature, some non-trivial spacetime solutions to the field equations exist that have either black hole [3] or cosmological event horizons [4, 5] when the cosmological constant is nonzero¹. Their metrics have the general form

$$(ds)^2 = -N^2(R)dT^2 + \frac{dR^2}{N^2(R)} + R^2(d\varphi + N^\varphi(R)dT)^2 \quad (1.1)$$

with the lapse (squared) and shift functions

$$N^2(R) = \frac{(\alpha_o R^2 + \gamma_o)(\alpha_i R^2 + \gamma_i)}{\ell^2 R^2}, \quad N^\varphi(R) = -\frac{\text{sign}(\alpha_o \alpha_i) \sqrt{\gamma_o \gamma_i}}{\ell R^2} \quad (1.2)$$

respectively. Here, $\alpha_{o/i}$ and $\gamma_{o/i}$ are constant parameters whose signs (and values) depend on whether we are considering the black hole solution in AdS space or the cosmological solution in dS space.

The ADM mass and angular momentum of this class of spacetimes, with a cosmological constant $\Lambda = \pm 1/\ell^2$, are given by

$$M_{BTZ} = \frac{R_o^2 + R_i^2}{8G\ell^2}, \quad J_{BTZ} = \frac{2R_o R_i}{8G\ell} \quad (1.3)$$

for the (BTZ) black hole solution (where $\alpha_o = \alpha_i = +1$, $\gamma_o = -R_o^2$, $\gamma_i = -R_i^2$) [3] and

$$M_{KdS_3} = \frac{R_o^2 - R_{(i)}^2}{8G\ell^2}, \quad J_{KdS_3} = \frac{2R_o R_{(i)}}{8G\ell} \quad (1.4)$$

for the (KdS₃) cosmological solution (where $\alpha_o = +1$, $\alpha_i = -1$, $\gamma_o = +R_o^2$, $\gamma_i = +R_{(i)}^2$) [4, 5], respectively², where the three-dimensional Newton constant G is assumed positive³. For the black hole case of Eq. (1.3), we have $M_{BTZ} \geq J_{BTZ}/\ell \geq 0$ in order that there is no naked conical singularity and $R_{o/i}$ denotes the *outer/inner* horizon. On the other hand, for the cosmological solution, there is no constraint on M_{KdS_3} and J_{KdS_3} in order that the horizon exists, unless $J_{KdS_3} = 0$ is considered [5]: Even $M_{KdS_3} < 0$ is allowed also. In this case, R_o denotes the

¹In general cosmological horizons in dS space do not necessarily imply the existence of black hole horizons in the associated AdS space. However, in three dimensions they are closely related, i.e, there is one-to-one correspondence between the “event” horizons – cosmological horizons in dS and outer black hole horizons in AdS – for overlapping ranges of ADM mass and angular momentum. See Ref. [5] for the details of the mapping.

²Here, mass and angular momentum agree with the definitions in Ref. [6] but differ in sign from Ref. [7].

³ In three-dimensional gravity, there is no *a priori* reason to fix the sign of Newton’s constant. For some recent discussion on the sign choice, see Ref. [2].

(cosmological) event horizon [4] but $R_{(i)}$ does not signify an inner horizon; the real parameter $R_{(i)}$ is introduced just for convenience [5].

Over the years black hole and cosmological solutions in three dimensions have fascinated theorists because of the potential insights they afford into quantum gravity. Amongst the most intriguing applications [9, 10, 11, 12] have been black hole formation and the associated issues of gravitational collapse and the cosmic censorship conjecture [8]. While there are numerous examples of initial conditions that form a naked singularity in the context of general relativity, none of them are generic as required by the terms of cosmic censorship conjecture. However it has been proposed that three dimensions might be an exception [13, 14]. A recent study of collapsing *shells* in three dimensions with *no* angular momentum showed that a naked singularity and a Cauchy horizon can form as the final result of shell collapse for a *broad* variety of initial data [10, 14]. This feature is quite generic since the results are independent of the types of collapsing shell matter such as pressureless dust, polytropic matter, and a generalized Chaplygin gas (GCG).

Furthermore, similar behaviour also appeared in previous studies of collapsing dust in three dimensions [9] and the formation of topological black holes in four dimensions [15]. (See refs. [11, 16] for higher-dimensional extensions.) The formation of a naked singularity is of great importance in association with the AdS/CFT correspondence [13, 17, 18] since one might ask whether or not the quantum correlation function at the AdS boundary is properly defined in the presence of a bulk singularity. This in turn raises additional issues associated with the collapse to a naked singularity, particularly the proper inclusion of quantum (gravity) effects in the bulk [19].

Thus far the possible scenarios for the emergence of a naked singularity have been explicitly analyzed for collapse to final states (black holes or otherwise) with no angular momentum [9, 10, 11, 12, 14, 15, 16]. Indeed, relatively little is explicitly known about the gravitational collapse of matter with nonzero angular momentum in any dimension. It is therefore natural to take into account an extension of gravitational collapse to exterior black holes with rotation (or other possible configurations) and to investigate how rotational effects alter previous results [9, 14] concerning cosmic censorship violation. While this problem is technically formidable in higher dimensions, a study of gravitational collapse of shells in three dimensions is considerably more tractable. So we shall consider this problem in our paper⁴.

To this end, we introduce a co-rotating coordinate system on the shell, which simplifies the matching procedure. The angular momentum produces a potential barrier around the origin, preventing the shell from contracting to zero size. We analyze the possible collapse scenarios by investigating the effective potential for all types of equation of state. For a pressureless dust shell, we find that its angular momentum prevents the creation of a singularity at the origin, unlike

⁴ After completing this work, a paper [20] investigating a rotating dust *cloud* appeared. Their “no singularity” result is consistent with our result for dust shells in Sec. 3. However, our results for shells with pressure in Sec. 4 imply that the naked singularity would *not* be avoided even for rotating clouds with pressure [21].

the non-rotating case [14]. Previous work on rotating dust shell collapse was carried out in the Hamiltonian formalism, an alternative to the Darmois-Israel formalism [22]. For a more restricted class of scenarios, they found that singularities were also avoided. Our work goes beyond this insofar as we consider shells with pressure. In this case, curvature singularities of finite spatial extent are formed before they meet the barrier, and the effective potential and surface stress-energy tensor diverge. Therefore under rather generic conditions it is possible for a naked singularity to form, violating cosmic censorship as in the non-rotating collapse scenario [14].

The outline of our paper is as follows. In Sec. 2, we present a set-up for the two-dimensional hypersurfaces with arbitrary rotations and a spherical symmetry. Considering a co-rotating frame where the co-moving observer on the shell sees only the radial motion yields a simplified equation of motion for the shell. In Sec. 3, we consider the evolution of a pressureless dust shell and compare it to the results for non-rotating shell collapse [14]. In Sec. 4, we consider shells with pressure whose equations of state are the polytrope type, which includes the perfect fluid and the GCG. Finally, we shall summarize and discuss our results in Sec. 5.

2 Set-up: Rotating Shells in Co-Rotating Frame

In this section, we consider rotating shells in three-dimensional Einstein gravity with a cosmological constant Λ . The bulk Einstein equation is given by

$$G_{\mu\nu} + \Lambda g_{\mu\nu} = 8\pi G T_{\mu\nu} \quad (2.1)$$

with a bulk stress-tensor $T_{\mu\nu}$. If we introduce a two-dimensional hypersurface with surface stress-energy tensor denoted by \mathcal{S}_{ij} , then the three-dimensional manifold is divided into three parts — the interior space \mathcal{V}_- , the exterior space \mathcal{V}_+ , and the thin-shell hypersurface Σ . The metric away from the shell decomposes as $g_{\mu\nu} = \Theta(\sigma)g_{\mu\nu}^+ + \Theta(-\sigma)g_{\mu\nu}^-$, where σ is a geodesic coordinate and $\Theta(\sigma)$ is the Heaviside step function⁵. We shall use the coordinate system (T, R, ϕ) in the interior and exterior spaces while we use the co-moving coordinate system (τ, ϕ) on the shell. Then, the evolution of the shell is obtained by the Darmois-Israel matching conditions between metrics and the corresponding extrinsic curvatures in the interior and the exterior geometries [23],

$$[g_{ij}] = 0, \quad (2.2)$$

$$8\pi G \mathcal{S}_{ij} = -([K_{ij}] - g_{ij}[K]) \quad (2.3)$$

where $[A] \equiv \lim_{\sigma \rightarrow 0}(A_+ - A_-)$ with the subscripts ‘+’ and ‘-’ denoting exterior and interior space-times, respectively. Greek letters (μ, ν, \dots) denote three-dimensional spacetime indices, whereas

⁵ $\Theta(\sigma)$ is equal to +1 if $\sigma > 0$, 0 if $\sigma < 0$, and indeterminate if $\sigma = 0$. It has the following properties : $\Theta^2(\sigma) = \Theta(\sigma)$, $\Theta(\sigma)\Theta(-\sigma) = 0$, and $d\Theta(\sigma)/d\sigma = \delta(\sigma)$, where $\delta(\sigma)$ is the Dirac delta function.

Roman letters (i, j, \dots) denote the two-dimensional indices on the shell. The combination of the metric junction condition and the induced Einstein's equation on the shell will describe the effective motion of the shell.

If we take a co-rotating frame on the shell by introducing $d\varphi = d\phi + \epsilon \frac{R_o R_i}{\ell \mathcal{R}^2(T)} dT$, then the metric (1.1) becomes

$$(ds)^2 = -N^2 dT^2 + \frac{dR^2}{N^2} + R^2 \left[d\phi + \frac{\epsilon R_o R_i}{\ell} \left(\frac{1}{\mathcal{R}^2(T)} - \frac{1}{R^2} \right) dT \right]^2 \quad (2.4)$$

and each metric in both regions is simply expressed as

$$(ds)_{\mathcal{V}_{\pm}}^2 = -N_{\pm}^2 dT^2 + \frac{dR^2}{N_{\pm}^2} + R^2 \left[d\phi - N_{\pm}^{\phi} R^2 \left(\frac{1}{\mathcal{R}^2(T)} - \frac{1}{R^2} \right) dT \right]^2, \quad (2.5)$$

with

$$N_{\pm}^2 = \frac{(\alpha_o^{\pm} R^2 + \gamma_o^{\pm})(\alpha_i^{\pm} R^2 + \gamma_i^{\pm})}{\ell^2 R^2}, \quad N_{\pm}^{\phi} = -\frac{\epsilon_{\pm} \sqrt{\gamma_o^{\pm} \gamma_i^{\pm}}}{\ell R^2} \quad (2.6)$$

and $\epsilon_{\pm} \equiv \text{sign}(\alpha_o^{\pm} \alpha_i^{\pm})$. Here $\alpha_{o/i}^{\pm}$ and $\gamma_{o/i}^{\pm}$ depend on the choice of spacetime. The black hole and cosmological solutions are respectively given by $\alpha_{o/i} = +1, \gamma_{o/i} < 0$ and $\alpha_o = -\alpha_i = +1, \gamma_o > 0$, as explained in Sec. 1. Note that T is a time (space) -like coordinate and R is a space (time) -like coordinate in the exterior (interior) of an outer black hole horizon or interior (exterior) of a cosmological horizon. Moreover, the horizonless geometry with point masses, where T is time-like and R is space-like always, corresponds to setting $\gamma_{o/i} > 0$ with $\alpha_{o/i} = +1$ for AdS space and $\alpha_i = 0, \alpha_o = +1$ for flat space [24].

On the shell's surface Σ with $T = \mathcal{T}(\tau)$ and $R = \mathcal{R}\mathcal{T}(\tau) = \mathcal{R}(\tau)$, the metric reduces to⁶

$$\begin{aligned} (ds)_{\Sigma}^2 &= -\mathcal{N}_{\pm}^2 d\mathcal{T}^2(\tau) + \frac{d\mathcal{R}^2(\tau)}{\mathcal{N}_{\pm}^2} + \mathcal{R}^2 d\phi^2 \\ &= g_{ij} dx^i dx^j \equiv -d\tau^2 + r_0^2 a^2(\tau) d\phi^2, \end{aligned} \quad (2.7)$$

which yields (from the first junction condition in Eq. (2.2))

$$\mathcal{N}_{\pm}^4 \left(\frac{d\mathcal{T}}{d\tau} \right)^2 = \left(\frac{d\mathcal{R}}{d\tau} \right)^2 + \mathcal{N}_{\pm}^2, \quad \mathcal{R}^2 = r_0^2 a^2(\tau). \quad (2.8)$$

The induced basis vectors and the normal vectors on Σ are

$$e_{\tau}^{\mu} = \left(\frac{d\mathcal{T}}{d\tau}, \frac{d\mathcal{R}}{d\tau}, 0 \right), \quad e_{\phi}^{\mu} = (0, 0, 1), \quad (2.9)$$

⁶ Here we consider the same cosmological constant parameter ℓ for both interior and exterior spacetimes. For the different parameters ℓ_{\pm} , the analysis is the same with the rescaled interior and exterior coordinates $\tilde{R}_{\pm} = R_{\pm} \ell / \ell_{\pm} = \mathcal{R}(\tau) \ell / \ell_{\pm}$, without changing the physical parameters α^{\pm} and γ^{\pm} .

and

$$n_\mu = \left(-\frac{d\mathcal{R}}{d\tau}, \frac{dT}{d\tau}, 0 \right), \quad (2.10)$$

respectively. Then, the non-vanishing components of the extrinsic curvature defined by $K_{ij} = -n_\alpha(\partial_j e_i^\alpha + \Gamma_{\mu\nu}^\alpha e_i^\mu e_j^\nu)$ are computed to be

$$K_{\tau\tau}^\pm = -\frac{d}{d\mathcal{R}} \sqrt{\left(\frac{d\mathcal{R}}{d\tau}\right)^2 + \mathcal{N}_\pm^2}, \quad K_{\tau\phi}^\pm = \frac{\text{sign}(\alpha_o^\pm \alpha_i^\pm) \sqrt{\gamma_o^\pm \gamma_i^\pm}}{\ell \mathcal{R}}, \quad K_{\phi\phi}^\pm = \mathcal{R} \sqrt{\left(\frac{d\mathcal{R}}{d\tau}\right)^2 + \mathcal{N}_\pm^2} \quad (2.11)$$

and its trace is

$$\begin{aligned} K &\equiv g^{ij} K_{ij} \\ &= \frac{d}{d\mathcal{R}} \sqrt{\left(\frac{d\mathcal{R}}{d\tau}\right)^2 + \mathcal{N}_\pm^2} + \frac{1}{\mathcal{R}} \sqrt{\left(\frac{d\mathcal{R}}{d\tau}\right)^2 + \mathcal{N}_\pm^2}. \end{aligned} \quad (2.12)$$

Note that $K_{\tau\phi}^\pm$ does not vanish even though there is no (T, ϕ) component of the metric on the shell where $R = \mathcal{R}(\tau)$, i.e., $f(R) \equiv -N^\phi R^2(1/\mathcal{R}^2(\tau) - 1/R^2) = 0$. This is basically because $\Gamma_{\tau\phi}^R$ has a term $\partial_R f(R)$ which does not vanish on the shell.

We shall assume that the surface stress-energy tensor of the shell is that of a perfect fluid

$$\mathcal{S}_{ij} = (\rho + p)u_i u_j + p g_{ij}, \quad (2.13)$$

where ρ is an energy density, p is a pressure, and u^i is the shell's two-velocity. Then, from the second junction condition (2.3), the surface stress-energy tensor with three-velocity $u^\mu = (1, 0, 0)$ is straightforwardly evaluated to be

$$\begin{aligned} -\rho &= \mathcal{S}^\tau_\tau = \frac{1}{8\pi G \mathcal{R}} (\beta_+ - \beta_-), \\ p &= \mathcal{S}^\phi_\phi = \frac{d}{8\pi G d\mathcal{R}} (\beta_+ - \beta_-), \end{aligned} \quad (2.14)$$

where $\beta_\pm \equiv \sqrt{(d\mathcal{R}/d\tau)^2 + \mathcal{N}_\pm^2}$. In addition, we have $\mathcal{S}_{\tau\phi} = (\rho + p)u_\tau u_\phi = 0$ since u_ϕ vanishes on the shell in the co-rotating frame. Hence $[K_{\tau\phi}] = 0$, which gives

$$K_{\tau\phi}^+ = \frac{\text{sign}(\alpha_o^+ \alpha_i^+) \sqrt{\gamma_o^+ \gamma_i^+}}{\ell \mathcal{R}} = \frac{\text{sign}(\alpha_o^- \alpha_i^-) \sqrt{\gamma_o^- \gamma_i^-}}{\ell \mathcal{R}} = K_{\tau\phi}^-, \quad (2.15)$$

implying $J_+ = J_-$ on the shell. Combining both equations in (2.14) yields

$$\beta_+ - \beta_- + 8\pi G \rho \mathcal{R} = 0, \quad (2.16)$$

$$\frac{d}{d\mathcal{R}}(\rho \mathcal{R}) + p = 0. \quad (2.17)$$

The first equation states that the (relativistic) energy of the shell, $2\pi\rho\mathcal{R}$ is balanced by the respective difference of energies $\beta_{\mp}/4G$, as measured from the interior and exterior spacetimes with given gravitational backgrounds. The second equation occurs because the shell is a closed, adiabatic system, with the loss of shell energy $d(2\pi\rho\mathcal{R})$ under expansion occurring at the expense of the work $2\pi p d\mathcal{R}$ done by the shell.

3 Pressureless Dust Shells

For a pressureless ($p = 0$) dust shell, Eq. (2.17) yields $\rho = m_0/2\pi\mathcal{R}$, where m_0 is an initial rest mass of the shell and is assumed to be a non-vanishing positive constant. Inserting this into Eq. (2.16) gives the equation of motion for the shell

$$\sqrt{\left(\frac{d\mathcal{R}}{d\tau}\right)^2 + \mathcal{N}_+^2} - \sqrt{\left(\frac{d\mathcal{R}}{d\tau}\right)^2 + \mathcal{N}_-^2} + 4Gm_0 = 0, \quad (3.1)$$

or alternatively

$$\left(\frac{d\mathcal{R}}{d\tau}\right)^2 + V_{\text{eff}}(\mathcal{R}) = 0, \quad (3.2)$$

where the effective potential is

$$V_{\text{eff}}(\mathcal{R}) = -\frac{1}{4(4Gm_0)^2} [(4Gm_0)^4 - 2(\mathcal{N}_+^2 + \mathcal{N}_-^2)(4Gm_0)^2 + (\mathcal{N}_+^2 - \mathcal{N}_-^2)^2]. \quad (3.3)$$

Note that this equation describes the one-dimensional Newtonian motion of a point particle with zero energy in the potential $V_{\text{eff}}(\mathcal{R})$ insofar as surfaces of constant τ are spacelike⁷. The behaviour of the shell will depend on the number of roots of the effective potential in $\mathcal{R} > 0$ [14].

Now if we define the dimensionless parameters (‘−’ for AdS and ‘+’ for dS)

$$x \equiv \mathcal{R}/\ell, \quad t \equiv \tau/\ell, \quad k_{o/i} \equiv \gamma_{o/i}/\ell^2 = \mp(x_{o/i})^2, \quad (3.4)$$

with the overdot denoting $\partial/\partial t$, then Eq. (3.2) becomes

$$\dot{x}^2 + V_{\text{eff}}(x) = 0, \quad (3.5)$$

where the effective potential is

$$V_{\text{eff}}(x) = \frac{1}{m_0^2 x^2} (a_8 x^6 + a_6 x^4 + a_4 x^2 + a_2) \quad (3.6)$$

⁷In the opposite case, when surfaces of constant \mathcal{R} are spacelike, the system corresponds to a non-conservative system with a time-dependent potential $V_{\text{eff}}(\mathcal{R})^{-1}$, due to absence of a time-like Killing vector. This situation is analogous to that of the S_0 -brane geometry [25]. For a related analysis in a S_0 -brane geometry, see Ref. [26].

and we employ henceforth the convention $8G \equiv 1$ for convenience, unless otherwise stated⁸. The coefficients are

$$\begin{aligned}
a_8 &= -(\alpha_o^+ \alpha_i^+ - \alpha_o^- \alpha_i^-)^2, \\
a_6 &= 2 \left[(\alpha_o^+ \alpha_i^+ + \alpha_o^- \alpha_i^-) m_0^2/4 - (\alpha_o^+ \alpha_i^+ - \alpha_o^- \alpha_i^-) (\alpha_o^+ k_i^+ + \alpha_i^+ k_o^+ - \alpha_i^- k_o^- - \alpha_o^- k_i^-) \right] \\
a_4 &= - \left[m_0^2/4 - (\alpha_o^+ k_i^+ + \alpha_i^+ k_o^+ + \alpha_i^- k_o^- + \alpha_o^- k_i^-) \right]^2 \\
&\quad + 4(\alpha_o^+ \alpha_o^- k_i^+ k_i^- + \alpha_i^+ \alpha_i^- k_o^+ k_o^- + \alpha_o^+ \alpha_i^- k_i^+ k_o^- + \alpha_o^- \alpha_i^+ k_o^+ k_i^-), \\
a_2 &= k_o^+ k_i^+ m_0^2 = k_o^- k_i^- m_0^2
\end{aligned}$$

with the condition $k_o^+ k_i^+ = k_o^- k_i^-$ ($J_+ = J_-$) on the shell from Eq. (2.15). Note that a non-vanishing coefficient a_8 implies the interior and exterior geometries differ; for example exterior AdS and interior dS spacetimes.

The coefficient a_2 , which is positive, is peculiar to geometries with rotation; if there is no rotation then a_2 vanishes ($k_i^\pm = 0$), and the effective potential agrees with that for the non-rotating case [14].

The effective potential can be classified by the values of its coefficients. For a non-vanishing a_8 (different geometries), the effective potential behaves as $V_{\text{eff}}(x) \approx a_2/m_0^2 x^2 \rightarrow +\infty$ as $x \rightarrow 0$ corresponding to a centrifugal barrier around the origin at $x = 0$. Hence the shell cannot collapse to zero size. We also have the asymptotic behaviour $V_{\text{eff}}(x) \approx a_8 x^4/m_0^2 \rightarrow -\infty$ as $x \rightarrow \infty$ since $a_8 < 0$. The shape of the effective potential is one of four types, depending on the values of the parameters (as illustrated in Fig. 1) and its numerator is a cubic polynomial in x^2 .

For vanishing a_8 , i.e., the same interior and exterior geometries, the numerator of the effective potential reduces to a quadratic polynomial in x^2 . The coefficient of the highest order term a_6 can have both positive and negative values, depending on the values of parameters, and the shapes of the effective potential are depicted in Fig. 2.

The crucial point concerning the different effective potentials depicted in Figs. 1 and 2 is the centrifugal barrier that appears around $x = 0$. It is this barrier that prevents the shell from contracting toward zero size, in turn preventing the formation of a curvature singularity at $x = 0$ unlike the non-rotating case [14].

We now turn to a discussion of exact solutions.

3.1 Exact Solutions I: Different Interior/Exterior Geometries ($a_8 \neq 0$).

We first consider the case of interior dS and exterior AdS spaces by setting $\alpha_{o/i}^+ = +1$, $\alpha_o^- = -\alpha_i^- = +1$, $M_+ = -(k_o^+ + k_i^+)$, $M_- = k_o^- - k_i^-$, $J = 2\ell\sqrt{k_o^\pm k_i^\pm}$, then we get

$$a_8 = -4,$$

⁸This differs from that of Ref. [14] by π .

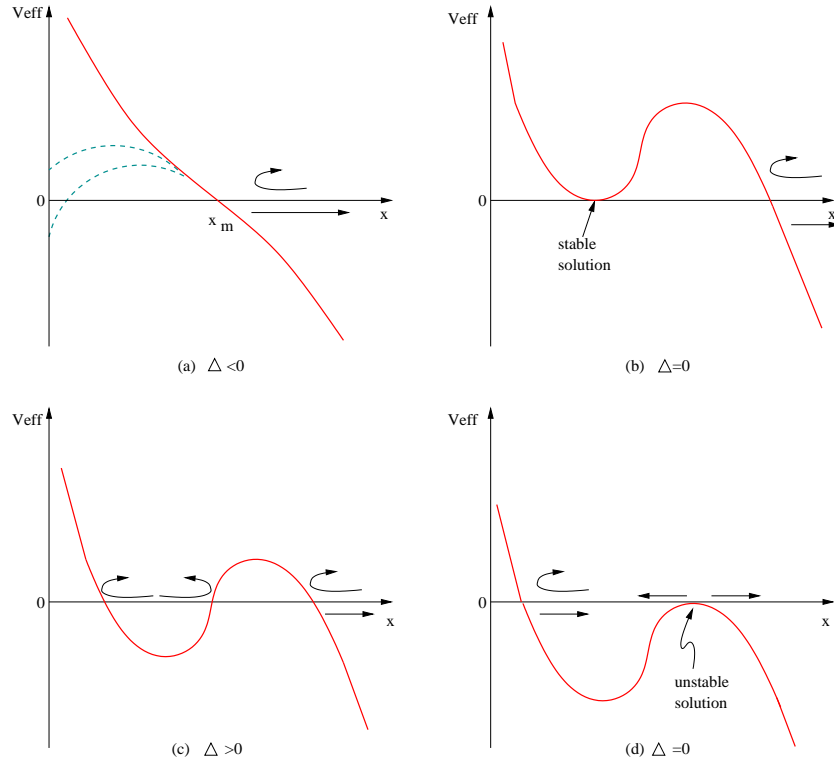


Figure 1: Plots of the effective potential for $a_8 < 0$ as a function of x . There are four cases: (a) a single root, (b) a degenerate small root and a large root, (c) three distinct roots, and (d) a degenerate large root and a small root. The arrows denote the possible trajectories of a shell with zero energy. The dotted lines denote the non-rotating cases ($a_2 = 0$), which exist only for $\Delta < 0$ defined in Eq. (3.17), and there are two types, depending on the value of a_4 . Note that there is a stable equilibrium solution located at the local minimum in (b), and an unstable equilibrium solution located at the local maximum in (d).

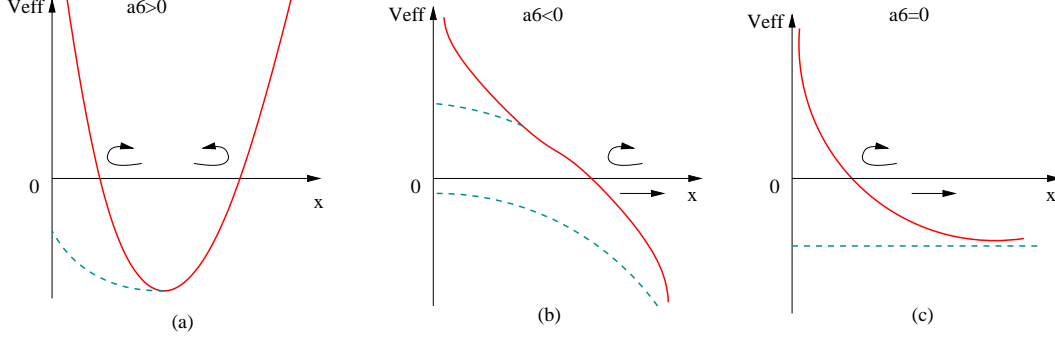


Figure 2: Plots of the effective potential as a function of x for $a_8 = 0$. The arrows denote the possible trajectories of a shell. The dotted lines denote the non-rotating case ($a_2 = 0$) and there can be two types, depending on the value of a_4 .

$$\begin{aligned}
a_6 &= 4(M_+ - M_-), \\
a_4 &= -(\mu_0^2 + M_+ + M_-)^2 + 4M_+M_-, \\
a_2 &= J_\pm^2 \mu_0^2 / \ell^2.
\end{aligned} \tag{3.7}$$

We can also reverse the above case by setting $\alpha_{o/i}^- = +1$, $\alpha_o^+ = -\alpha_i^+ = +1$, $M_- = -(k_o^- + k_i^-)$, $M_+ = k_o^+ - k_i^+$, $J = 2\ell\sqrt{k_o^\pm k_i^\pm}$, and easily find that the coefficients are obtained by switching ‘+’ \leftrightarrow ‘-’, as expected due to the corresponding symmetry in the configuration.

Next consider an interior dS and exterior flat space. This corresponds to setting $\alpha_o^+ = +1$, $\alpha_i^+ = 0$, $\alpha_o^- = -\alpha_i^- = +1$, $m_+ = 2(1 - \sqrt{k_i^+})$, $j_+ = 2\ell\sqrt{k_o^+}$, $M_- = k_o^- - k_i^-$, $J_- = 2\ell\sqrt{k_o^- k_i^-}$, which reduces the coefficients to

$$\begin{aligned}
a_8 &= -1, \\
a_6 &= -\left[\frac{m_0^2}{2} + \frac{1}{2}(m_+ - 2)^2 + 2M_-\right], \\
a_4 &= -\left[\frac{m_0^2}{4} - \frac{1}{4}(m_+ - 2)^2 + M_-\right]^2 - (m_+ - 2)^2 M_-, \\
a_2 &= \frac{1}{16\ell^2}(m_+ - 2)^2 j_+^2 m_0^2 = \frac{J_-^2 m_0^2}{4\ell^2}.
\end{aligned} \tag{3.8}$$

In the last line, we have used the junction condition $k_o^+ k_i^+ = k_o^- k_i^-$ and this shows that it is not the angular momentum j_+ itself but the combination $(2 - m_+)j_+/2$ (with m_+ the mass parameter of the exterior locally flat space) that is continuous across the shell and matches with the angular momentum J_- of the interior dS space. Note that the case of interior AdS and exterior flat spaces can be similarly obtained by changing $a_6 \rightarrow -a_6$ in the above formula with $M_- = -(k_o^- + k_i^-)$. Reversing the interior and exterior spaces can be obtained by switching ‘+’ \leftrightarrow ‘-’.

Eq. (3.5) is not a particularly convenient form for obtaining an exact solution. Rather, by introducing $X \equiv x^2$, we find that (3.5) can be rewritten as

$$\dot{X}^2 + \hat{V}_{\text{eff}}(X) = 0, \quad (3.9)$$

where

$$\hat{V}_{\text{eff}}(X) \equiv 4XV_{\text{eff}}(x) = \frac{4}{m_0^2}(a_8X^3 + a_6X^2 + a_4X + a_2). \quad (3.10)$$

Since the effective potential can be rewritten in the form ($a > 0$)

$$\hat{V}_{\text{eff}}(X) = -\frac{4}{m_0^2}a(X-b)(X-c)(X-d), \quad (3.11)$$

where $a_8 = -a$, $a_6 = a(b+c+d)$, $a_4 = -a(bd+bc+cd)$, and $a_2 = abcd$, one finds that the differential equation has an exact solution in terms of the Jacobi elliptic function⁹

$$\begin{aligned} t - \mathcal{C} &= -\frac{m_0}{\sqrt{a(d-b)}} \text{JacobiSN}^{-1} \left[\sqrt{\frac{x^2-b}{c-b}}, \sqrt{\frac{c-b}{d-b}} \right] \\ &= \frac{m_0}{\sqrt{a(d-b)}} \text{EllipticF} \left[\sqrt{\frac{x^2-b}{c-b}}, \sqrt{\frac{c-b}{d-b}} \right], \end{aligned} \quad (3.12)$$

which can be rewritten as

$$x(t) = \left[b + (c-b) \text{JacobiSN}^2 \left\{ \frac{\sqrt{a(d-b)}}{m_0}(t-\mathcal{C}), \sqrt{\frac{c-b}{d-b}} \right\} \right]^{1/2}. \quad (3.13)$$

The integration constant \mathcal{C} is

$$\begin{aligned} \mathcal{C} &= \frac{m_0}{\sqrt{a(d-b)}} \text{JacobiSN}^{-1} \left[\sqrt{\frac{x_0^2-b}{c-b}}, \sqrt{\frac{c-b}{d-b}} \right] \\ &= \frac{m_0}{\sqrt{a(d-b)}} \text{EllipticF} \left[\sqrt{\frac{x_0^2-b}{c-b}}, \sqrt{\frac{c-b}{d-b}} \right] \end{aligned} \quad (3.14)$$

determined by setting $x = x_0$ at $t = 0$.

The three roots b, c, d can be rewritten as

$$r_0 = s_+ + s_- - \frac{a_6}{3a_8}, \quad r_{\pm} = -\frac{1}{2}(s_+ + s_-) - \frac{a_6}{3a_8} \pm i\frac{\sqrt{3}}{2}(s_+ - s_-), \quad (3.15)$$

where $s_{\pm} = \sqrt[3]{r \pm i\sqrt{q^3 - r^2}}$ with

$$r = \frac{9a_8a_6a_4 - 27a_8^2a_2 - 2a_6^3}{54a_8^3}, \quad q = \frac{-3a_8a_4 + a_6^2}{9a_8^2} \quad (3.16)$$

⁹The properties of the Jacobi elliptic functions are presented in Refs. [14, 27].

and here the choice of identification of $\{r_0, r_\pm\}$ with $\{b, c, d\}$ is arbitrary. For $a_8 \neq 0$, the number of “real” roots depends on the discriminant

$$\begin{aligned}\Delta &\equiv 108a_8^4(q^3 - r^2) \\ &= -27a_2^2a_8^2 + 2a_4(9a_6a_2 - 2a_4^2)a_8 + a_6^2(a_4^2 - 4a_6a_2).\end{aligned}\quad (3.17)$$

If $\Delta > 0$, there are three distinct real roots and if $\Delta = 0$, (at least) two roots coincide, while if $\Delta < 0$, there is only one real root with a pair of complex conjugate roots (Fig. 1). Plugging Eq. (3.7) into Eq. (3.17) yields

$$\begin{aligned}\Delta &= -27\mu_0^{12} - 162\mu_0^{10}z - 54\mu_0^8(y^2 + 6z^2) - 54\mu_0^6(4(zy^2 + z^3) - 9J^2y) \\ &\quad - 27\mu_0^4(y^4 + 8z^2y^2 + 27J^4 - 36J^2zy) - 54\mu_0^2(zy^4 - J^2y^3)\end{aligned}\quad (3.18)$$

with $\mu_0 \equiv m_0/2$, $y \equiv M_+ - M_-$, and $z \equiv M_+ + M_-$.

Thus we conclude that collapse scenarios with different interior and exterior geometries (see Fig. 1) are described by the exact solution of Eq. (3.13), with parameters appropriately chosen. Note that for the non-rotating case ($J = 0$ and $z > 0$) $\Delta < 0$ always (Fig. 1 (a)). The crucial difference between the rotating case and the non-rotating case [14] is the centrifugal barrier around the origin that prevents the shell from collapsing to zero size, forbidding the formation of a curvature singularity for the former. This is manifest in Eq. (3.18), where we can see that the effect of rotation gives *positive* contributions for $y > 0$, and so can render Δ non-negative (Fig. 1 (b), (c), and (d)).

3.2 Exact Solutions II: Same Interior/Exterior Geometries ($a_8 = 0$).

For the same interior and exterior geometries we have $a_8 = 0$. The solutions become simpler in that they can be expressed by trigonometric or exponential functions. To see this, we first consider AdS spaces in both regions by setting $\alpha_{o/i}^\pm = +1$. Then we get

$$\begin{aligned}a_8 &= 0, \quad a_6 = m_0^2, \\ a_4 &= -[m_0^2/4 - (k_o^+ + k_i^+ + k_o^- + k_i^-)]^2 + 4(k_o^+ + k_i^+)(k_o^- + k_i^-), \\ a_2 &= k_o^+ k_i^+ m_0^2\end{aligned}\quad (3.19)$$

with the condition $k_o^+ k_i^+ = k_o^- k_i^-$. Alternatively, if we define the mass and angular momentum parameters $M_\pm \equiv -(k_o^\pm + k_i^\pm)$ and $J \equiv 2\ell\sqrt{k_o^\pm k_i^\pm}$, then the black hole and the AdS point mass spacetimes can be described by $M > 0$ and $M < 0$, respectively, and one finds

$$V_{\text{eff}}(x) = \frac{m_0^2 x^4 - \tilde{a}_4 x^2 + m_0^2 J^2 / 4\ell^2}{m_0^2 x^2}, \quad (3.20)$$

where $\tilde{a}_4 \equiv -a_4$ is positive definite when at least one of the interior/exterior geometries is a black hole geometry. For example for BTZ black holes in both regions ($M_{\pm} > 0$), we have $\tilde{a}_4 = m_0^4/16 + m_0^2(M_+ + M_-)/2 + (M_+ - M_-)^2 > 0$. Likewise for interior AdS point mass and exterior BTZ black hole case ($M_+M_- < 0$) we have $\tilde{a}_4 = (m_0^2/4 + M_+ + M_-)^2 - 4M_+M_- > 0$. However for AdS point masses in both regions, \tilde{a}_4 cannot be positive always.

The shape of the effective potential is given in Fig. 2 (a) since $a_6 = 4\mu_0^2 > 0$. So there are two positive roots at $x = x_{\min/\max}$, where

$$x_{\min} = \frac{\sqrt{\tilde{a}_4 - \sqrt{\tilde{a}_4^2 - m_0^4 J^2/\ell^2}}}{\sqrt{2}m_0}, \quad x_{\max} = \frac{\sqrt{\tilde{a}_4 + \sqrt{\tilde{a}_4^2 - m_0^4 J^2/\ell^2}}}{\sqrt{2}m_0}. \quad (3.21)$$

and the shell moves between them as illustrated in Fig. 2 (a). An exact solution can be found by a straightforward computation:

$$t - \mathcal{C} = -\frac{1}{2} \arctan \left[\frac{\tilde{a}_4 - 2m_0^2 x^2}{2\sqrt{-m_0^4 x^4 + \tilde{a}_4 m_0^2 x^2 - m_0^2 J^2/\ell^2}} \right]. \quad (3.22)$$

Alternatively we can write

$$x(t) = \frac{1}{\sqrt{2}m_0} \left[\tilde{a}_4 + \sqrt{\tilde{a}_4^2 - m_0^4 J_+^2} |\sin 2(t - \mathcal{C})| \right]^{1/2} \quad (3.23)$$

or

$$x(t) = \frac{1}{\sqrt{2}} \left[(x_{\max}^2 + x_{\min}^2) + (x_{\max}^2 - x_{\min}^2) |\sin 2(t - \mathcal{C})| \right]^{1/2}, \quad (3.24)$$

where the integration constant \mathcal{C} is determined by an initial condition on the position of the shell $x_0 \equiv x(t=0)$,

$$\mathcal{C} = \frac{1}{2} \arctan \left[\frac{\tilde{a}_4 - 2m_0^2 x_0^2}{2\sqrt{-m_0^4 x_0^4 + \tilde{a}_4 m_0^2 x_0^2 - m_0^2 J^2/\ell^2}} \right]. \quad (3.25)$$

It is clear that a (real) solution exists only for $\tilde{a}_4 > 0$: For AdS point masses in both regions, i.e., $M_{\pm} < 0$, we need particular initial configurations satisfying $m_0^2/4 > 2\sqrt{M_+M_-} - (M_+ + M_-)$ or $m_0^2/4 < -2\sqrt{M_+M_-} - (M_+ + M_-)$ in order to have real solutions.

Note that the minimum bound at $x = x_{\min}$ arises due to the angular momentum parameter J , which implies that the shell will not shrink to zero size. The intrinsic Ricci scalar on the shell computed from the induced metric (2.4),

$$\mathcal{R}_{\mu}^{\mu}[\Sigma] = \frac{2}{x(t)} \frac{d^2 x(t)}{dt^2} = -\frac{1}{x} \frac{dV_{\text{eff}}}{dx}, \quad (3.26)$$

has no singularity since the shell cannot reach the origin at $x = 0$ due to the angular momentum barrier. This implies that rotational effects prevent the curvature singularity at $x = 0$ from being formed.

Formation of a BTZ black hole will take place if certain initial conditions hold. First the inequalities $x_{\max} \geq x_0 > x_H^+ > x_{\min}$ must hold, so that the shell's initial location is outside of the putative horizon x_H^+ of the exterior spacetime, which in turn must be located between x_{\min} and x_{\max} . A BTZ black hole can form for the exterior observer before the shell moving inward either collapses *onto* the interior point mass, collapses *into* a point mass if the interior is pure AdS, or is absorbed into the outer horizon of an interior BTZ black hole¹⁰.

To see this, consider Eq. (3.1), which can be written as

$$\frac{m_0}{2} = \sqrt{\dot{x}^2 + x^2 + \frac{J^2}{4\ell^2 x^2} - M_-} - \sqrt{\dot{x}^2 + x^2 + \frac{J^2}{4\ell x^2} - M_+} \quad (3.27)$$

and note that everything in the square-root terms is the same except for M_+ and M_- .

If there is a black hole in the interior spacetime, i.e., $M_- > 0$, then a black hole in the exterior spacetime, i.e., $M_+ > 0$, will always form for a positive m_0 , for any initial point x_0 : The shell moving inward forms the (outer) black hole horizon before being absorbed by the outer horizon of the interior black hole, i.e., $x_H^- < x_H^+$ which is equivalent to $M_- < M_+$.

If the interior is pure AdS or has a point mass, i.e., $M_- < 0$, then a black hole in the exterior spacetime ($M_+ > 0$) forms if

$$\bar{m}_0 < m_0 \quad (3.28)$$

with $\bar{m}_0/2 = \sqrt{\dot{x}_0^2 + \mathcal{N}_-^2(x_0)} - \sqrt{\dot{x}_0^2 + \mathcal{N}_+^2(x_0) + M_+}$, for any initial point x_0 .

For $m_0 < \bar{m}_0$ then $M_+ < 0$ and the shell collapses into (or onto) a point mass, which is similar to the condition for dust *cloud* collapse in the non-rotating case [9]. Furthermore, for $0 < m_0 < \bar{m}_0$ we have $0 > M_+ > M_-$; the deficit angle, which is defined by $2\pi(1 - \sqrt{-M_{\pm}})$ [24], of the point mass outside can not be smaller than that of the point mass inside. Note that the physics governing the endstate of collapse is basically the same regardless of the values of \dot{x}_0 and J .

On the other hand, by squaring (3.1) one find that the shell's gravitational mass M_+ , which becomes the black hole mass after its formation, is given by

$$M_+ = m_0 \sqrt{\dot{x}^2 + \mathcal{N}_-^2} - 2Gm_0^2 + M_-, \quad (3.29)$$

(reinstating Newton's constant G) where the first and second terms correspond to the shell's relativistic kinetic energy and binding energy, respectively [28]. Note that the binding energy is negative only for *positive* G , as in the conventional higher dimensional black holes [30]¹¹; this is unique to AdS spacetimes and this could provide a physical explanation of why the black hole solution can exist only in this case, but not in dS or flat spacetimes.

¹⁰ The formation of a black hole would also occur for interior flat or AdS point mass spacetime provided appropriate conditions are met.

¹¹ Constant binding energy is peculiar to three dimensions; in general there is distance dependence. In four dimensions, for example, the gravitational mass of a spherically symmetric shell, with a flat interior spacetime, is given by $M_+ = m_0 \sqrt{\dot{x}^2 + 1} - G_4 m_0^2 / 2R$ with G_4 the four-dimensional Newton's constant.

Next we consider dS spaces in both regions by setting $\alpha_o^\pm = +1$ and $\alpha_i^\pm = -1$. Then we get

$$\begin{aligned} a_8 &= 0, \quad a_6 = -m_0^2, \\ a_4 &= -[m_0^2/4 + (k_o^+ - k_i^+ + k_o^- - k_i^-)]^2 + 4(k_o^+ - k_i^+)(k_o^- - k_i^-), \\ a_2 &= k_o^+ k_i^+ m_0^2 \end{aligned} \quad (3.30)$$

with the condition $k_o^+ k_i^+ = k_o^- k_i^-$. The effective potential is ($\tilde{a}_4 \equiv -a_4 > 0$)

$$V_{\text{eff}}(x) = \frac{-m_0^2 x^4 - \tilde{a}_4 x^2 + m_0^2 J^2 / 4\ell^2}{m_0^2 x^2}. \quad (3.31)$$

In this case, the shape of the effective potential is Fig. 2(b) since $a_6 = -m_0^2 < 0$ with a single root at $x = x_{\min}$, where

$$x_{\min} = \frac{\sqrt{-\tilde{a}_4 + \sqrt{\tilde{a}_4^2 + m_0^4 J^2 / \ell^2}}}{\sqrt{2} m_0} \quad (3.32)$$

provided $J = 2\ell\sqrt{k_o^\pm k_i^\pm} \neq 0$; for vanishing angular momentum ($J = 0$), i.e., non-rotating dS spaces, there is no x_{\min} (the lower dotted line in Fig. 2(b)). The solution for the shell's edge is

$$x(t) = \frac{1}{2m_0} \sqrt{\frac{1}{\ell^2} m_0^2 J^2 e^{2(t-C)} + \left[m_0 e^{-(t-C)} - \frac{\tilde{a}_4}{m_0} e^{(t-C)} \right]^2}, \quad (3.33)$$

where the integration constant C is

$$C = -\frac{1}{2} \ln \left[\frac{8m_0^2 x_0^2 + 4\tilde{a}_4 + 8m_0 \sqrt{m_0^2 x_0^4 + \tilde{a}_4 x_0^2 - m_0^2 J^2 / 4\ell^2}}{m_0^2} \right]. \quad (3.34)$$

As with black hole spacetimes, when some appropriate conditions are imposed, a (cosmological) event horizon x_C^- can form from the perspective of the interior observer. If the cosmological horizon x_C^- of the interior spacetime is located larger than x_{\min} and if the initial location of the dust shell is in between x_{\min} and x_C^- , the expanding (or collapsing and later expanding) shell will form a cosmological horizon for the interior (KdS₃) observer.

To see this explicitly, we note that, as in the black hole case, the cosmological horizons are located always larger than x_{\min} ¹², i.e., $x_{\min} \leq x_C^\pm = \sqrt{k_o^\pm}$, from $\tilde{a}_4 + m_0^2 M_\pm = (m_0/2)^4 + m_0^2 (M_\mp + 3M_\pm)/2 + (M_+ - M_-)^2 \geq 0$ for any non-zero μ_0 . Regardless of the sign of $(M_+ + 3M_-)$ this condition is trivially satisfied since there are no real values of μ_0 satisfying $\tilde{a}_4 + m_0^2 M_\pm < 0$.

Consider again Eq. (3.1), which we write as

$$\frac{m_0}{2} = \sqrt{\dot{x}^2 + M_- + \frac{J^2}{4\ell^2 x^2}} - x^2 - \sqrt{\dot{x}^2 + M_+ + \frac{J^2}{4\ell x^2}} - x^2. \quad (3.35)$$

¹²This can be also understood from (3.2) which is always satisfied when the shell's location coincides with one of the horizons, i.e., $\mathcal{N}_+ = 0$ or $\mathcal{N}_- = 0$.

Note that the contributions of the mass terms M_{\pm} are opposite to those of the black hole spacetime due to our definition of mass [5, 6]. Then the expanding (or collapsing and later expanding) shell will form a cosmological horizon for the interior (KdS₃) observer for a *negative* m_0 : If $m_0 > 0$, then $x_C^- > x_C^+$, which is equivalent to $M_+ > M_-$, and the shell will be absorbed by the cosmological horizon of the exterior spacetime, before forming the cosmological horizon in the interior spacetime¹³.

Finally we consider flat spaces in both regions by setting $\alpha_i^{\pm} = 0$ and $\alpha_o^{\pm} = +1$. We have

$$\begin{aligned} a_8 &= a_6 = 0, \\ a_4 &= -[m_0^2/4 - (k_i^+ + k_i^-)]^2 + 4k_i^+ k_i^-, \\ a_2 &= k_o^+ k_i^+ m_0^2 \end{aligned} \quad (3.36)$$

with the condition $k_o^+ k_i^+ = k_o^- k_i^-$. If we define the mass and angular momentum parameters m^{\pm} and j^{\pm} of the point masses to be $k_i^{\pm} = (m_{\pm} - 2)^2/4$, $k_o^{\pm} = j_{\pm}^2/4\ell^2$, then one finds the effective potential becomes

$$V_{\text{eff}}(x) = \frac{-\tilde{a}_4 x^2 + (16\ell^2)^{-1}(m_{\pm} - 2)^2 j_{\pm}^2 m_0^2}{m_0^2 x^2}, \quad (3.37)$$

where $\tilde{a}_4 \equiv -a_4 = [m_0^2/4 - (k_i^+ + k_i^-)]^2 - 4k_i^+ k_i^-$. Its shape is shown in Fig. 2(c), since $a_6 = 0$ with a single root at $x = x_{\min}$, where

$$x_{\min} = \frac{|(m_{\pm} - 2)j_{\pm}|m_0}{4\ell\sqrt{\tilde{a}_4}}. \quad (3.38)$$

Here we note that the angular momenta j_{\pm} are not separately continuous across the shell, but only the combinations $(m_{\pm} - 2)j_{\pm}$ are. The exact solution is found to be

$$x(t) = \frac{m_0|(m_{\pm} - 2)j_{\pm}|}{4\ell\sqrt{\tilde{a}_4}} \sqrt{1 + \frac{16\tilde{a}_4^2 \ell^2}{(m_{\pm} - 2)^2 j_{\pm}^2 m_0^4} (t - \mathcal{C})^2}, \quad (3.39)$$

where the integration constant \mathcal{C} is

$$\mathcal{C} = \frac{m_0}{2\tilde{a}_4} \sqrt{4\tilde{a}_4 x_0^2 - (m_{\pm} - 2)^2 j_{\pm}^2 m_0^2/4\ell}. \quad (3.40)$$

To summarize this section, we find that rotating dust shells can collapse, but only down to a minimal size x_{\min} (after which they expand) due to their angular momentum. No curvature singularity is formed during the gravitational collapse process, unlike the non-rotating case [14]. The alternative collapse endpoint is a BTZ black hole or a KdS₃ spacetime.

¹³ In the non-rotating case this scenario has been previously noted in a higher-dimensional context [18].

4 Shells with Pressure

In this section, we shall consider shells with pressure determined by somewhat generalized equations of state. The effect of pressure is to produce a varying shell energy $2\pi\ell\rho x$ from Eq. (2.17), i.e., deviations from the inverse radius dependence of $\rho = m_0/2\pi\ell x$. Specifically we consider shells with the polytropic-type equation of state

$$p = \frac{\omega\rho}{\pi} \left(\frac{2\pi\ell\rho}{m_0} \right)^{1/n}, \quad (4.1)$$

that encompasses many sorts of known fluids by choosing a specific equation of state parameter ω and polytropic index n . For instance, we have constant energy density ($n = 0$), non-relativistic degenerate fermions ($n = 1$), non-relativistic matter or radiation pressure ($n = 2$), and linear (perfect) fluid ($n \rightarrow \infty$), respectively [29]. Moreover, the equation of state in Eq. (4.1) can describe a Chaplygin gas by choosing $n, \omega < 0$.

Plugging the equation of state (4.1) into Eq. (2.17) yields

$$\rho(x) = \frac{m_0}{2\pi\ell} \left(-\omega + \mu x^{1/n} \right)^{-n}, \quad (4.2)$$

where μ is an integration constant. Similarly, for the linear fluid ($n \rightarrow \infty$), we have

$$\rho(x) = \frac{m_0}{2\pi\ell} x^{-(\omega+1)}. \quad (4.3)$$

From these we obtain the equations

$$\sqrt{\dot{x}^2 + \mathcal{N}_+^2} - \sqrt{\dot{x}^2 + \mathcal{N}_-^2} + \frac{(m_0 x/2)}{(-\omega + (1 + \omega)x^{1/n})^n} = 0, \quad (4.4)$$

for finite n , and

$$\sqrt{\dot{x}^2 + \mathcal{N}_+^2} - \sqrt{\dot{x}^2 + \mathcal{N}_-^2} + \frac{(m_0/2)}{x^\omega} = 0, \quad (4.5)$$

for the linear fluid, where $\mu = 1 + \omega$ so that $\rho = m_0/2\pi\ell$ when $x = 1$.

For finite n and the linear fluid, the equations of motion can be expressed in the alternate form

$$\dot{x}^2 + V_{\text{eff}}(x) = 0, \quad (4.6)$$

where the effective potential is

$$V_{\text{eff}}(x) = \frac{1}{2}(\mathcal{N}_+^2 + \mathcal{N}_-^2) - \frac{\pi^2\ell^2}{4}\rho^2 x^2 - \frac{1}{4\pi^2\ell^2\rho^2 x^2}(\mathcal{N}_+^2 - \mathcal{N}_-^2)^2 \quad (4.7)$$

with the junction condition $k_o^+ k_i^+ = k_o^- k_i^-$. Note that the only change to the effective potential compared to pressureless dust shells in Eq. (3.3) is the replacement of $m_0 \rightarrow 2\pi\ell\rho x$ in Eq. (3.3).

Up to now, the preceding results are valid for any n . But the behaviour of the effective potential differs for $n > 0$ and $n < 0$, which need separate consideration.

4.1 The Ordinary Polytopic Shells: $n, \omega > 0$

For ordinary fluids with finite and positive definite n and ω , the effective potential and the intrinsic Ricci scalar also *negatively* diverge at $x = x_\omega \equiv \omega^n/(1 + \omega)^n$, where the density ρ also diverges. So the shell will not collapse to a point but rather to a ring of finite size $x = x_\omega$ in a finite proper time. The shape of the effective potential is depicted in Figs. 3 and 4.

On the other hand, for the linear fluid ($n \rightarrow \infty$) there is no ring singularity since ρ is finite for any finite x . Rather, from the effective potential near $x = 0$,

$$V_{\text{eff}} \approx \frac{J^2}{4\ell^2 x^2} - \frac{m_0^2}{16x^{2\omega}} + \frac{1}{2}(\alpha_i^+ k_o^+ + \alpha_o^+ k_i^+ + \alpha_i^- k_o^- + \alpha_o^- k_i^-) - \frac{x^{2\omega}}{m_0^2}(\alpha_i^+ k_o^+ + \alpha_o^+ k_i^+ - \alpha_i^- k_o^- - \alpha_o^- k_i^-)^2, \quad (4.8)$$

due to $\rho(x) = (m_0/2\pi\ell)x^{-(\omega+1)}$, a shell with $\omega > 1$ will collapse to zero size¹⁴, *regardless of* the initial values of m_0 and $k_o^\pm k_i^\pm \equiv J^2/4\ell^2$, in a finite proper time where the effective potential and the energy density (or pressure) diverge (Figs. 5 and 6).

Provided the exterior geometry has no black hole (event) horizon such as the KdS₃ space or the AdS/flat spaces with point masses, there is nothing to prevent the collapsing shell from developing a curvature singularity. The resultant singularity is naked and we have a violation of the cosmic censorship for “generic” initial data. These are qualitatively the same behaviours as those of non-rotating shell collapse [14], which implies that their angular momentum is not large enough to overcome forming the curvature singularity for most fluids whose equations of state are of the form (4.1). The centrifugal barrier that prevents collapse in the pressureless dust case still occurs at $x = 0$, but is always dominated by the negatively divergent effective potential at the finite value of x .

However, for the linear fluid with $\omega < 1$, angular momentum effects again dominate, ensuring that cosmic censorship is upheld regardless of the relative values of m_0 and J (Figs. 7 and 8). Note that this is the case where there is a similarity with the pressureless dust shells in Sec. 3: Actually, Figs. 7 and 8 (and Fig. 10 as well) show all the possible cases in Figs. 1 and 2.

The case $\omega = 1$ is a marginal case that crucially depends on the initial data: One has an infinite well for $m_0^2 > 4J^2$ (Fig. 9) but an infinite barrier for $m_0^2 < 4J^2$ (Fig. 10); for $m_0^2 = 4J^2$, the point $x = 0$ is naked when $(\alpha_i^+ k_o^+ + \alpha_o^+ k_i^+ + \alpha_i^- k_o^- + \alpha_o^- k_i^-) < 0$ (Fig. 11).

¹⁴ The case $\omega < -1$ shows similar behaviour for the effective potential and $\omega = -1$ is a marginal case. We shall not consider these possibilities, i.e., $\omega < 0$ with the usual values of $n > 0$, since their physical relevance is not quite clear.

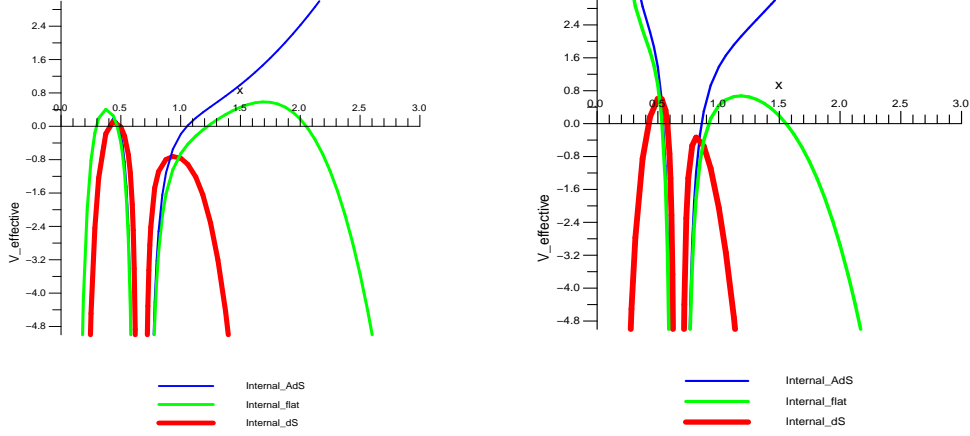


Figure 3: Plots of the effective potentials for the shell with a polytropic equation of state and the exterior AdS black hole ($\alpha_{o/i}^+ = +1, k_o^+ = -(x_H^+)^2 = -1, k_i^+ = -1/4$: LHS)/AdS point mass ($\alpha_{o/i}^+ = +1, k_o^+ = +1, k_i^+ = +1/4$: RHS). We choose an interior AdS space with a point mass ($\alpha_i^- = +1$), flat ($\alpha_i^- = 0$), and dS ($\alpha_i^- = -1$) by setting parameters $\alpha_o^- = +1, \omega = +2, k_{o/i}^- = +1/2, m_0 = 4, n = +1$.

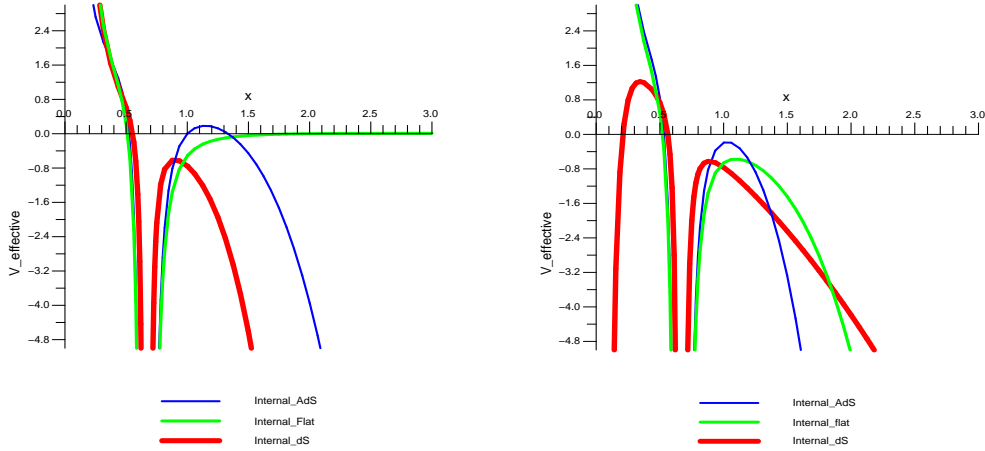


Figure 4: Plots of the effective potentials for the shell with a polytropic equation of state and the exterior flat space ($\alpha_o^+ = 0, \alpha_i^+ = +1, k_o^+ = +1, k_i^+ = +1/4$: LHS)/dS space ($\alpha_o^+ = +1, \alpha_i^- = -1, k_o^+ = (x_C^+)^2 = +1, k_i^+ = +1/4$: RHS). We choose an interior AdS space with a point mass ($\alpha_i^- = +1$), flat ($\alpha_i^- = 0$), and dS ($\alpha_i^- = -1$) by setting parameters $\alpha_o^- = +1, \omega = +2, k_{o/i}^- = +1/2, m_0 = 2, n = +1$.

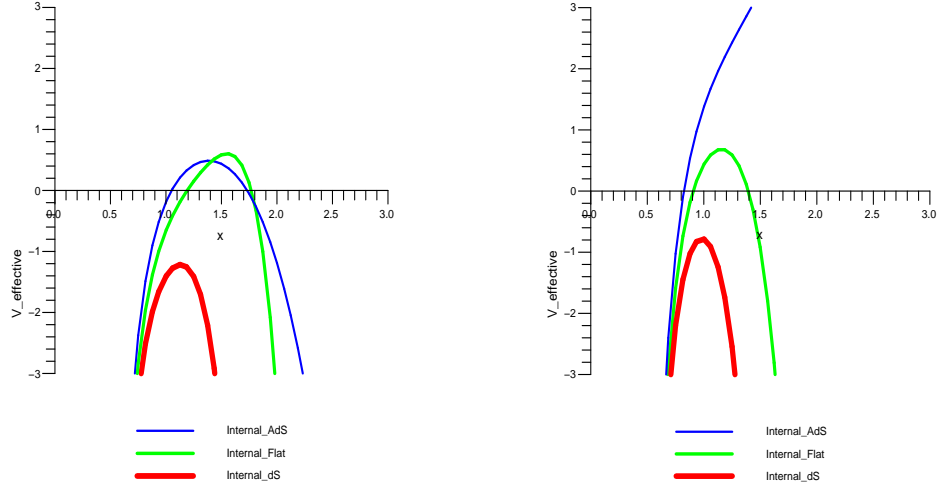


Figure 5: Plots of the effective potentials for the shell with a linear fluid and the exterior AdS black hole ($k_o^+ = -(x_H^+)^2 = -1, k_i^+ = -1/4$: LHS)/AdS point mass ($k_o^+ = +1, k_i^+ = +1/4$: RHS). We choose an interior AdS space with a point mass ($\alpha_i^- = +1$), flat ($\alpha_i^- = 0$), and dS ($\alpha_i^- = -1$) by setting parameters $\alpha_o^- = +1, \omega = +2, k_{o/i}^- = +1/2, m_0 = 4$.

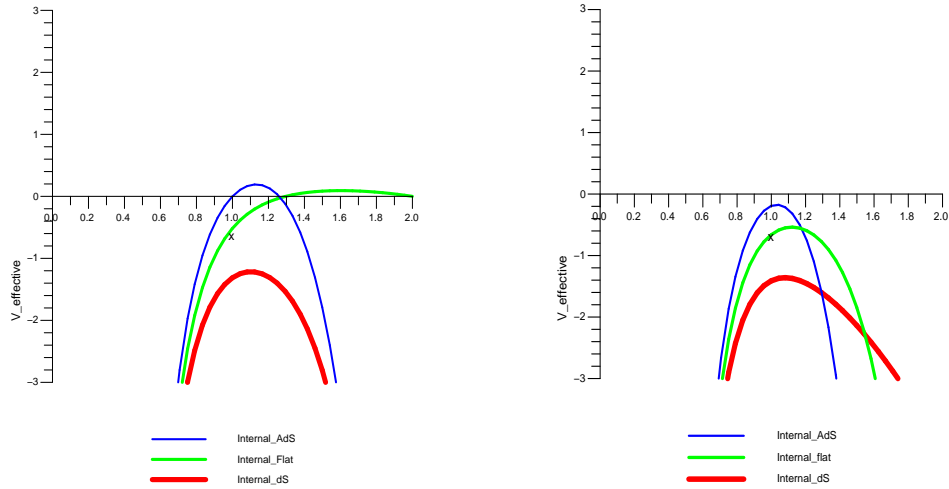


Figure 6: Plots of the effective potentials for the shell with a linear fluid and the exterior flat space ($\alpha_o^+ = 0, \alpha_i^+ = +1, k_o^+ = +1, k_i^+ = +1/4$: LHS)/dS space ($\alpha_o^+ = +1, k_o^+ = (x_C^+)^2 = +1, k_i^+ = +1/4$: RHS). We choose an interior AdS space with a point mass ($\alpha_i^- = +1$), flat ($\alpha_i^- = 0$), and dS ($\alpha_i^- = -1$) by setting parameters, $\alpha_o^- = +1, \omega = +2, k_{o/i}^- = +1/2, m_0 = 4$.

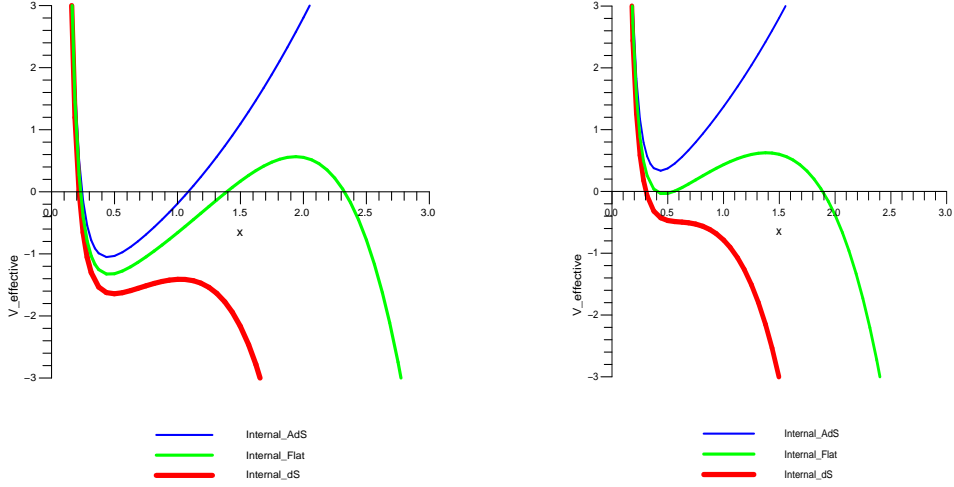


Figure 7: Plots of the effective potentials for the shell with a linear fluid and the exterior AdS black hole ($k_o^+ = -(x_H^+)^2 = -1, k_i^+ = -1/4$: LHS)/AdS point mass ($k_o^+ = +1, k_i^+ = +1/4$: RHS). We choose an interior AdS space with a point mass ($\alpha_i^- = +1$), flat ($\alpha_i^- = 0$), and dS ($\alpha_i^- = -1$) by setting parameters $\alpha_o^- = +1, \omega = +1/2, k_{o/i}^- = +1/2, m_0 = 4$. The event horizon for the exterior observer is located at $x = 1.0$ in the left diagram. However a fluid collapsing through this surface will not bounce from the interior barrier.

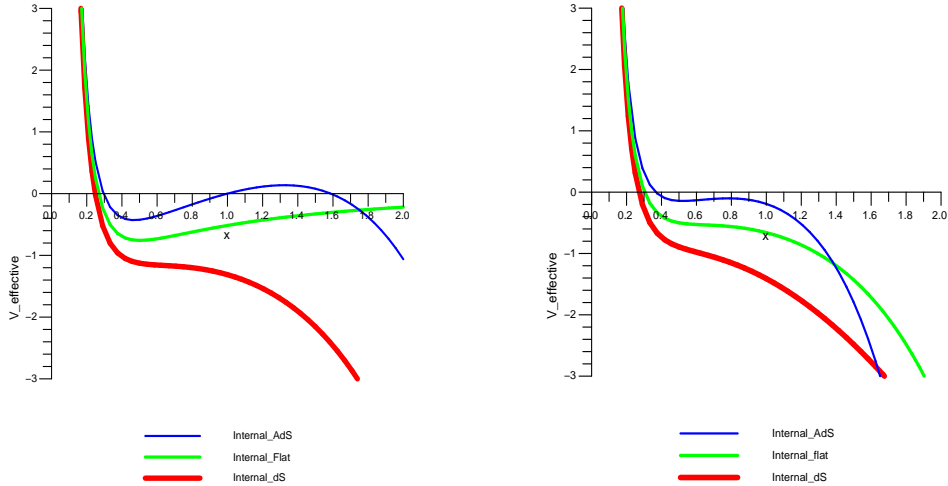


Figure 8: Plots of the effective potentials for the shell with a linear fluid and the exterior flat space ($\alpha_o^+ = 0, \alpha_i^+ = +1, k_o^+ = +1, k_i^+ = +1/4$: LHS)/dS space ($\alpha_{o/i}^+ = +1, k_o^+ = (x_C^+)^2 = +1, k_i^+ = +1/4$: RHS). We choose an interior AdS space with a point mass ($\alpha_i^- = +1$), flat ($\alpha_i^- = 0$), and dS ($\alpha_i^- = -1$) by setting parameters, $\alpha_o^- = +2, \omega = +1/2, k_{o/i}^- = +1/2, m_0 = 4$.

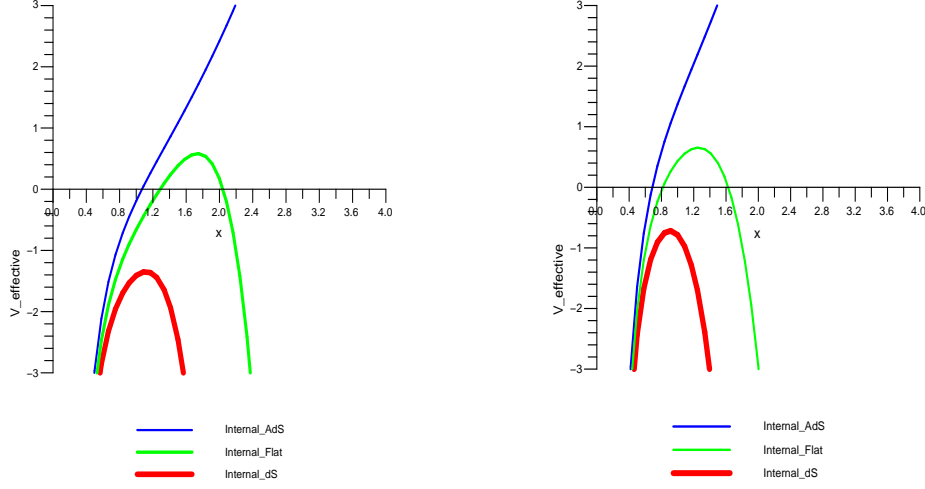


Figure 9: Plots of the effective potentials for the shell with a linear fluid and the exterior AdS black hole ($k_o^+ = -(x_H^+)^2 = -1, k_i^+ = -1/4$: LHS)/AdS point mass ($k_o^+ = +1, k_i^+ = +1/4$: RHS). We choose an interior AdS space with a point mass ($\alpha_i^- = +1$), flat ($\alpha_i^- = 0$), and dS ($\alpha_i^- = -1$) by setting parameters $\alpha_o^- = +1, \omega = +1, k_{o/i}^- = +1/2, m_0 = 4$.

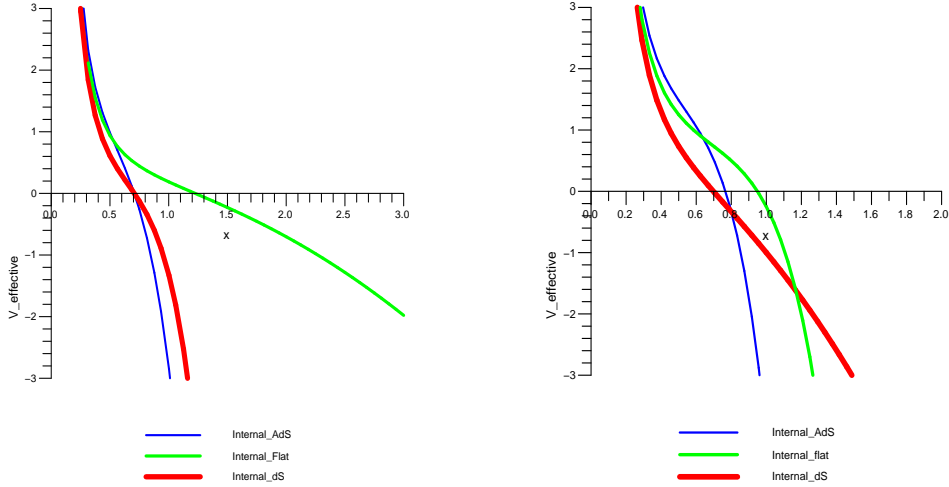


Figure 10: Plots of the effective potentials for the shell with a linear fluid and the exterior flat space ($\alpha_o^+ = 0, \alpha_i^+ = +1, k_o^+ = +1, k_i^+ = +1/4$: LHS)/dS space ($\alpha_o^+ = +1, k_o^+ = (x_C^+)^2 = +1, k_i^+ = +1/4$: RHS). We choose an interior AdS space with a point mass ($\alpha_i^- = +1$), flat ($\alpha_i^- = 0$), and dS ($\alpha_i^- = -1$) by setting parameters, $\alpha_o^- = +1, \omega = +1, k_{o/i}^- = +1/2, m_0 = 1$.

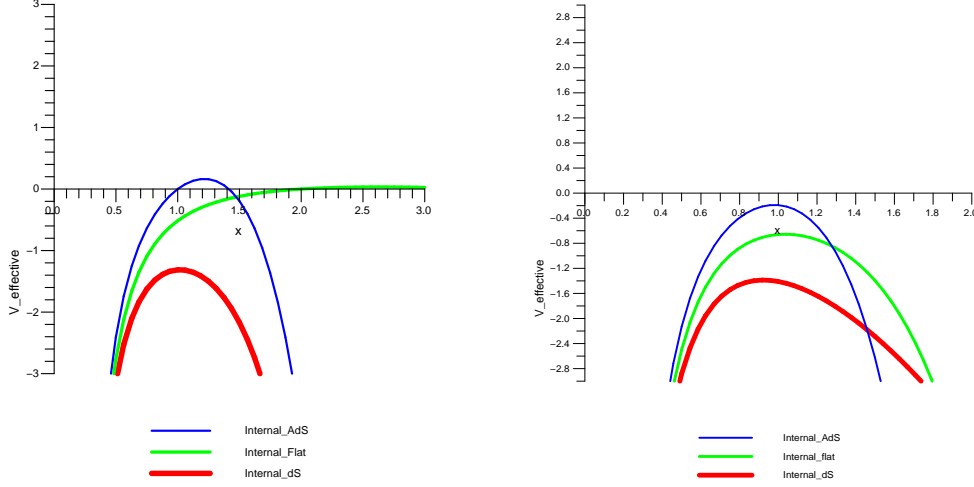


Figure 11: Plots of the effective potentials for the shell with a linear fluid and the exterior flat space ($\alpha_o^+ = 0, \alpha_i^+ = +1, k_o^+ = +1, k_i^+ = +1/4$: LHS)/dS space ($\alpha_{o/i}^+ = +1, k_o^+ = (x_C^+)^2 = +1, k_i^+ = +1/4$: RHS). We choose an interior AdS space with a point mass ($\alpha_i^- = +1$), flat ($\alpha_i^- = 0$), and dS ($\alpha_i^- = -1$) by setting parameters, $\alpha_o^- = +1, \omega = +1, k_{o/i}^- = +1/2, m_0 = 4$.

4.2 Chaplygin-Gas Shells: $n, \omega < 0$

For the Chaplygin-type gas shells ($n, \omega < 0$), by setting $n = -1/(\lambda+1)$ one can conveniently rewrite the equation of state¹⁵ as $p = -\hat{A}/\pi\rho^\lambda = -A(m_0/2\pi^2\ell)(m_0/2\pi\ell\rho)^\lambda$ and $\omega = -\hat{A}(m_0/2\pi\ell)^{1/n} = -A$, in agreement with more standard conventions [31]. Then, for finite n , i.e., $\lambda \neq -1$ one finds

$$\rho(x) = \frac{m_0}{2\pi\ell} \left[A + (1-A)x^{-(\lambda+1)} \right]^{1/(\lambda+1)}, \quad (4.9)$$

from Eq. (4.2).

The shape of the effective potential depends on several parameters A , $\alpha_{o/i}^\pm$, and $k_{o/i}^\pm$, as shown in Fig. 12. Near $x = 0$, the effective potential behaves as

$$V_{\text{eff}}(x) \approx \frac{1}{4} \frac{J^2/\ell^2}{x^2} - \frac{m_0^2(1-A)^2}{16} - \frac{(\alpha_i^+ k_o^+ + \alpha_o^+ k_i^+ - \alpha_i^- k_o^- - \alpha_o^- k_i^-)^2}{m_0^2(1-A)^2} \quad (4.10)$$

due to $\rho(x) \approx (m_0/2\pi\ell)(1-A)$ for $A \neq 1$, from Eq. (4.9). Again there is a centrifugal barrier near the origin. The asymptotic behaviour as $x \rightarrow \infty$ is given by

$$V_{\text{eff}}(x) \approx \frac{1}{2} \left[(\alpha_o^+ \alpha_i^+ + \alpha_o^- \alpha_i^-) - \frac{1}{16} m_0^2 A^{2/(\lambda+1)} \right] x^2 \quad (4.11)$$

¹⁵For a close connection to D-branes, see Ref. [32].

and this depends on the values of A and $\alpha_{o/i}^\pm$, similarly to Fig. 2. In addition, as can be seen from a consideration of the effective potential (4.7), it will not diverge for any finite value of x when $A < 1$, while it will *negatively* diverge due to the vanishing energy density, i.e., $\rho \rightarrow 0$ at $x = x_A \equiv [(A - 1)/A]^{1/(\lambda+1)}$ when $A > 1$ for all $\lambda > -1$.

On the other hand, for $A = 1$, we have a uniform density $\rho(x) = m_0/2\pi\ell$ from Eq. (4.9) also and the (full) effective potential is given by

$$V_{\text{eff}}(x) = \frac{1}{2}(\mathcal{N}_+^2 + \mathcal{N}_-^2) - \frac{1}{16}m_0^2x^2 - \frac{1}{m_0^2x^2}(\mathcal{N}_+^2 - \mathcal{N}_-^2)^2. \quad (4.12)$$

Near $x = 0$, this behaves as

$$V_{\text{eff}}(x) \approx \frac{1}{4} \frac{J^2/\ell^2}{x^2} - \frac{(\alpha_i^+ k_o^+ + \alpha_o^+ k_i^+ - \alpha_i^- k_o^- - \alpha_o^- k_i^-)^2}{m_0^2 x^2} - \frac{m_0^2}{16} \quad (4.13)$$

and it depends on initial data: One has an infinite well for $J^2 < 4\ell^2(\alpha_i^+ k_o^+ + \alpha_o^+ k_i^+ - \alpha_i^- k_o^- - \alpha_o^- k_i^-)^2/m_0^2$ (this is what has been plotted in Fig. 12), and an infinite barrier for $J^2 > 4\ell^2(\alpha_i^+ k_o^+ + \alpha_o^+ k_i^+ - \alpha_i^- k_o^- - \alpha_o^- k_i^-)^2/m_0^2$. The case $J^2 = 4\ell^2(\alpha_i^+ k_o^+ + \alpha_o^+ k_i^+ - \alpha_i^- k_o^- - \alpha_o^- k_i^-)^2/m_0^2$ is a marginal case that has a finite well and a finite intrinsic curvature; the intrinsic curvature is finite even at the point $x = 0$, from Eq. (3.26)¹⁶, and so $x = 0$ is a bounce point. As $x \rightarrow \infty$, the effective potential behaves as

$$V_{\text{eff}}(x) \approx \left[\frac{1}{2}(\alpha_o^+ \alpha_i^+ + \alpha_o^- \alpha_i^-) - \frac{m_0^2}{16} - \frac{1}{m_0^2}(\alpha_o^+ \alpha_i^+ - \alpha_o^- \alpha_i^-)^2 \right] x^2 \quad (4.14)$$

which depends on the initial data also.

As an explicit example, we consider $\lambda = 1$, describing a conventional Chaplygin gas shell [31]. Then the effective potential becomes

$$V_{\text{eff}}(x) = \frac{1}{m_0^2(Ax^2 + 1 - A)x^2}(a_8x^6 + a_6x^4 + a_4x^2 + a_2), \quad (4.15)$$

where

$$\begin{aligned} a_8 &= -[m_0^4 A^2/16 - (\alpha_o^+ \alpha_i^+ + \alpha_o^- \alpha_i^-)(m_0/2)^4 A/2 + (\alpha_o^+ \alpha_i^+ - \alpha_o^- \alpha_i^-)^2], \\ a_6 &= -m_0^4 A(1 - A)/8 + [(\alpha_o^+ k_i^+ + \alpha_i^+ k_o^+ + \alpha_i^- k_o^- + \alpha_o^- k_i^-)A + (\alpha_o^+ \alpha_i^+ + \alpha_o^- \alpha_i^-)(1 - A)] m_0^2/2 \\ &\quad - 2(\alpha_o^+ \alpha_i^+ - \alpha_o^- \alpha_i^-)(k_i^+ \alpha_o^+ + \alpha_i^+ k_o^+ - \alpha_i^- k_o^- - \alpha_o^- k_i^-), \\ a_4 &= -m_0^4(1 - A)^2/16 + [(\alpha_o^+ k_i^+ + \alpha_i^+ k_o^+ + \alpha_o^- k_i^- + \alpha_i^- k_o^-)(1 - A) + 2k_o^- k_i^- A] m_0^2/2 \\ &\quad - (\alpha_o^+ k_i^+ + \alpha_i^+ k_o^+ + \alpha_i^- k_o^- + \alpha_o^- k_i^-)^2 \\ &\quad + 4(\alpha_o^+ \alpha_o^- k_i^+ k_i^- + \alpha_i^+ \alpha_i^- k_o^+ k_o^- + \alpha_o^+ \alpha_i^- k_i^+ k_o^- + \alpha_o^- \alpha_i^+ k_o^+ k_i^-), \\ a_2 &= m_0^2 k_o^- k_i^- (1 - A). \end{aligned}$$

¹⁶ The only relevant term is the x^2 term (omitted in (4.13)), which cancels the $1/x$ factor in Eq. (3.26).

For a black hole spacetime outside the shell, the collapsing shell may form a black hole within a finite time for $A \leq 1$. But this is not always the case for $A > 1$ since there exists a singular point at $x = x_A = \sqrt{(A-1)/A}$. If the horizon x_H is located at $x_H > x_A$, then it will form a black hole, while if $x_H < x_A$, it will form a finite-sized ring singularity unless the numerator vanishes at the point x_A , $a_8 x_A^6 + a_6 x_A^4 + a_4 x_A^2 + a_2 = 0$. Apart from a contrivance of very restrictive conditions on the parameters $m_0, \alpha_{o/i}^\pm, k_{o/i}^\pm$, and A , this is still a somewhat singular configuration: even though the intrinsic Ricci scalar of the shell is finite and its energy density vanishes, the pressure diverges at the point x_A . This suggests a bounce solution.

Comparing to the non-rotating case [14], we again find that angular momenta does not in general prevent the emergence of a naked ring singularity at a finite position of $x = x_A$. Violation of cosmic censorship occurs from the gravitational shell collapse, regardless of the rotation and initial data.

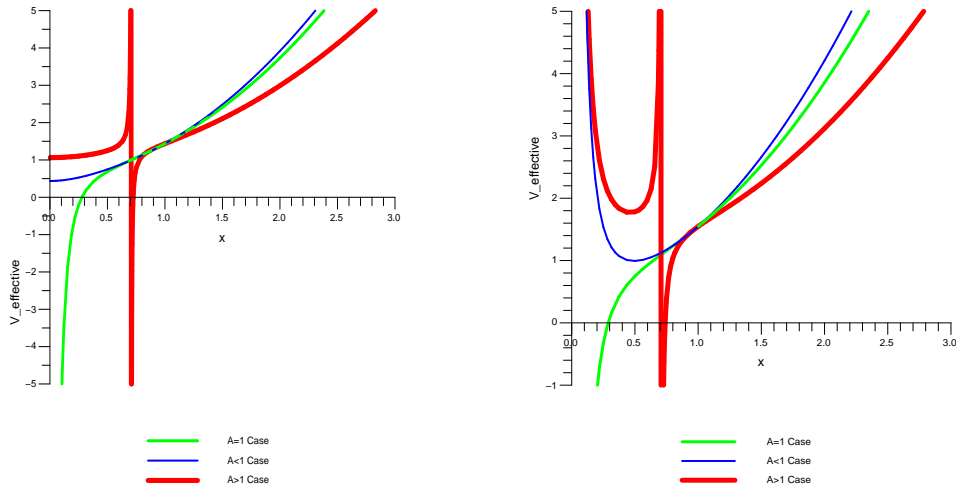


Figure 12: Plots of the effective potentials for the GCG shell with $\lambda = 1$ and the exterior/interior AdS spaces with point masses ($\alpha_{o/i}^\pm = +1, k_o^+ = +1, k_i^+ = +1/4, k_{o/i}^- = +1/2, m_0 = 2$). (1) LHS: the case of non-rotating shell (2) RHS: the case of rotating shell.

5 Discussion

Our investigation of the gravitational collapse of rotating shells in three dimensions has uncovered a number of interesting features. We have studied whether or not angular momentum can significantly change the collapse scenario and its resulting cosmic censorship violations in the non-rotating cases in the literature.

For asymptotically AdS boundary conditions, we find that the rotating shell collapses to either a black hole or a minimum value and then expands out to infinity. For shells composed of pressureless dust these are the only scenarios; the centrifugal barrier forbids a naked singularity from forming. However for shells with pressure we have another scenario in which a naked singular ring can form, violating cosmic censorship. When the exterior spacetime is taken to be a geometry with a point mass, one might expect that the collapsing shell could form a curvature singularity within finite time, since there is no event horizon as with the non-rotating system in Ref. [14]. However we have shown that a naked singularity never forms in the collapse of a rotating dust shell due to a centrifugal barrier in the effective potential experienced by the shell. Collapse scenarios for shells with pressure show that a naked ring singularity of finite size can be formed, where the effective potential and the surface stress-energy tensor diverge. For asymptotically dS boundary conditions a collapsing shell with pressure can form a naked singularity, also. If the interior spacetime is (K)dS, then a cosmological horizon can form from an expanding shell. Which of these scenarios occurs depends on the choice of parameters and initial conditions.

For asymptotically flat boundary conditions the qualitative behaviours are similar, *i.e.*, a rotating collapsing dust shell does not form a naked singularity, but a shell with pressure can form a naked singularity. For a polytropic shell this will be a naked singular ring of finite size. The qualitative behaviour is more or less intermediate between the asymptotically AdS and dS cases as implied by the choice of $\alpha_{o/i}^{\pm}$ and illustrated in Figs. 4 and 7, though there are some anomalous regions that do not reveal this simple trend.

The most intriguing lesson of this paper is that the centrifugal barrier in the effective potential governing the time evolution of a rotating dust shell can prevent formation of a naked singularity. However if the shell has pressure, a ring singularity may form for a typical class of equations of state, *i.e.*, $\omega > 1$, where the pressure dominates the angular momentum, with quite general initial data. So if the exterior spacetime is assumed to be a geometry without a (covered) black hole event horizon, then the singularity may be naked and the violation of cosmic censorship is possible.

We have found that a collapsing shell can form either a black hole/cosmological horizon or a naked singularity or bounce to infinity, depending on the initial data. This suggests a set of phase transitions [10] along with accompanying critical phenomena, similar to that discovered for scalar matter [33]. It would be of great interest to study these phenomena explicitly as they could reveal universal features of the critical exponents in three dimensions.

Since we have confined our study to three dimensions (where there is no gravitational radiation), some caution is warranted in applying our results to higher dimensions. We have found that the angular momentum does not in general prevent violation of cosmic censorship in three dimensions, where local gravitational interactions vanish outside of matter. An interesting extension of our work would be to include higher derivative terms, whose effect is to produce such interactions.

Another interesting extension is the inclusion of quantum effects, since they might be expected to prevent singularity formation, thereby sidestepping the cosmic censorship issue. What impact these modifications have on our results remains to be investigated.

Acknowledgment

We would like to thank Sang Pyo Kim and Shin Nakamura for exciting discussions and the head-quarter of APCTP for warm hospitality during the APCTP-TPI Joint Focus Program and Workshop. J. J. Oh would like to thank Wontae Kim, Seungjoon Hyun, Hongbin Kim, Jaehoon Jeong, Hyeong Chan Kim, Gungwon Kang, Inyong Cho, Constantinos Papageorgakis, Andrew Strominger, and Chi-Ok Hwang for useful and helpful discussions. R. B. Mann was supported by the Natural Sciences and Engineering Research Council of Canada. J. J. Oh was supported by the Korea Research Council of Fundamental Science & Technology (KRCF). M.-I. Park was supported by the Korea Research Foundation Grant funded by Korea Government(MOEHRD) (KRF-2007-359-C00011).

References

- [1] S. Deser, R. Jackiw, and G. 't Hooft, *Ann. Phys. (N.Y.)* **152**, 220 (1984).
- [2] S. Deser, R. Jackiw, and S. Templeton, *Ann. Phys. (N.Y.)*, **140**, 372 (1982); W. Li, W. Song, and A. Strominger, *JHEP* **0804**, 082 (2008); S. Carlip, S. Deser, A. Waldron, and D. K. Wise, [arXiv:0803.3998 \[hep-th\]](#); D. Grumiller and N. Johansson, *JHEP* **0807**, 134 (2008); M.-I. Park, *JHEP* **0809**, 084 (2008); I. Sachs and S. N. Solodukhin, *JHEP* **0808**, 003 (2008); D. Grumiller, R. Jackiw and N. Johansson, [arXiv:0806.4185 \[hep-th\]](#).
- [3] M. Bañados, C. Teitelboim, and J. Zanelli, *Phys. Rev. Lett.* **69**, 1849 (1992); M. Bañados, M. Henneaux, C. Teitelboim, and J. Zanelli, *Phys. Rev. D* **48**, 1506 (1993).
- [4] S. Deser and R. Jackiw, *Ann. Phys. (N.Y.)* **153**, 405 (1984).
- [5] M.-I. Park, *Phys. Lett. B* **440**, 275 (1998); D. Klemm and L. Vanzo, *JHEP* **0204**, 030 (2002); M.-I. Park, *Class. Quantum Grav.* **25**, 135003 (2008).
- [6] V. Balasubramanian, J. de Boer and D. Minic, *Phys. Rev. D* **65**, 123508 (2002); Y. S. Myung, *Mod. Phys. Lett. A* **16**, 2353 (2001); A. M. Ghezelbash and R. B. Mann, *JHEP* **0201**, 005 (2002).
- [7] A. Strominger, *JHEP* **0110**, 034 (2001); D. Klemm, *Nucl. Phys. B* **625**, 295 (2002).
- [8] R. Penrose, *Riv. Nuovo Cim.* **1**, 252 (1969) [*Gen. Rel. Grav.* **34**, 1141 (2002)].

- [9] R. B. Mann and S. F. Ross, Phys. Rev. D **47**, 3319 (1993).
- [10] A. Peleg and A. R. Steif, Phys. Rev. D **51**, R3992 (1995).
- [11] A. Ilha, A. Kleber, and J. P. S. Lemos, J. Math. Phys. **40**, 3509 (1999).
- [12] S. Gutti, Class. Quantum Grav. **22**, 3233 (2005).
- [13] V. E. Hubeny, X. Liu, M. Rangamani and S. Shenker, JHEP **0412**, 067 (2004).
- [14] R. B. Mann and J. J. Oh, Phys. Rev. D **74**, 124016 (2006) [Erratum-ibid. D **77**, 129902 (2008)].
- [15] W. L. Smith and R. B. Mann, Phys. Rev. D **56**, 4942 (1997).
- [16] A. Ilha and J. P. S. Lemos, Phys. Rev. **D55**, 1788 (1997); R. Goswami and P. S. Joshi, Phys. Rev. D **69**, 044002 (2004); J. Crisostomo, S. del Campo and J. Saavedra, Phys. Rev. D **70**, 064034 (2004); R. Tibrewala, S. Gutti, T. P. Singh and C. Vaz, Phys. Rev. D **77**, 064012 (2008).
- [17] T. Hertog, G. T. Horowitz and K. Maeda, Phys. Rev. D **69**, 105001 (2004); K. Copsey and R. B. Mann, JHEP **0805**, 069 (2008).
- [18] B. Freivogel, V. E. Hubeny, A. Maloney, R. Myers, M. Rangamani, and S. Shenker, JHEP **0603**, 007 (2006).
- [19] S. Gutti and T. P. Singh, Phys. Rev. D **76**, 064026 (2007); C. Vaz, S. Gutti, C. Kiefer and T. P. Singh, Phys. Rev. D **76**, 124021 (2007); C. Vaz, S. Gutti, C. Kiefer, T. P. Singh and L. C. R. Wijewardhana, Phys. Rev. D **77**, 064021 (2008).
- [20] C. Vaz and K. R. Koehler, Phys. Rev. D **78**, 024038 (2008).
- [21] R. B. Mann, J. J. Oh and M.-I. Park, in preparation.
- [22] J. Crisostomo and R. Olea, Phys. Rev. D **69**, 104023 (2004).
- [23] W. Israel, Nuovo Cimento B **44**, 1 (1966); J. E. Chase, Nuovo Cimento B **67**, 136 (1970).
- [24] S. Carlip, “Quantum Gravity in 2+1 Dimensions” (Cambridge University Press, Cambridge, UK, 1998).
- [25] M. Gutperle and A. Strominger, JHEP **0204**, 018 (2002).
- [26] C. P. Burgess, P. Martineau, F. Quevedo, G. Tasinato and I. Zavala, JHEP **0303**, 050 (2003).

- [27] M. Abramowitz and I. A. Stegun, *Handbook of Mathematical Functions* (Dover, New York, 1970).
- [28] E. Poisson, “A Relativist’s Toolkit: The Mathematics of Black-Hole Mechanics” (Cambridge University Press, Cambridge, England, 2004).
- [29] N. J. Cornish and N. E. Frankel, Phys. Rev. D **43**, 2555 (1991).
- [30] R. C. Myers and M. J. Perry, Annals Phys. **172**, 304 (1986).
- [31] S. Chaplygin, Sci. Mem. Moscow Univ. Math. Phys. **21**, 1 (1904); A. Kamenshchik, U. Moschella, and V. Pasquier, Phys. Lett. B **511**, 265 (2001); N. Bilic, G. B. Tupper, and R. D. Viollier, Phys. Lett. B **535**, 17 (2002); M. C. Bento, O. Bertolami, and A. A. Sen, Phys. Rev. D **66**, 043507 (2002).
- [32] R. Jackiw and A. P. Polychronakos, Commun. Math. Phys. **207**, 107 (1999); R. Jackiw, arXiv:physics/0010042.
- [33] D. Birmingham and S. Sen, Phys. Rev. Lett. **84**, 1074 (2000); F. Pretorius and M. Choptuik, Phys. Rev. D **62**, 124012 (2000); D. Garfinkle, Phys. Rev. D **63**, 044007 (2001); V. Husain and M. Olivier, Class. Quantum Grav. **18**, L1 (2001).